

# CAN FD system design

Dr.-Ing. M. Schreiner – Daimler Research and Development

**Abstract – The objective of this paper is to give general design rules for the physical layer of CAN FD networks. As an introduction influencing parameters are analyzed and physical relationships are shown. Critical values of typical components are given. The main section will then present a systematical analysis of basic CAN FD topologies (e.g. star, bus or sub topology). The topologies will be described by geometrical parameters and the respective physical characteristics will be derived. Finally an assessment of the possible baud rates of given network topologies as a function of the geometrical parameters will be provided.**

## Introduction

After its introduction in 2012 [1] CAN FD quickly turned out to be the next big thing for in vehicle networking in addition to the introduction of automotive Ethernet. Meanwhile CAN FD has become a new ISO standard and many automakers are about to integrate CAN FD into the next generation of their vehicles [4], [5]. One of the main benefits of the new CAN FD protocol is its ability to transmit the data phase of the frame with higher speed. Under lab conditions even 10 Mbits/s and more have been demonstrated for small networks.

The ability of CAN or CAN FD to run on nearly any kind of network topology is its strength and weakness at the same time. Many CAN users have gained experience in designing Classical CAN networks at 125 kbit/s ... 500 kbit/s but up to now may do not have a feeling for the appropriate baud rate of a CAN FD topology. The focus of the paper is to give an overview about the characteristics of frequently used CAN topologies in terms of CAN FD data phase speed. The results given in this paper enable CAN users to determine the maximum baud rate of frequently used topologies for save operation under mass production.

## Design rules for Classical CAN

Classical CAN is also a basic part of CAN FD (bus access etc.) and hence when designing a CAN FD network the rules for proper arbitration, acknowledge etc. must not be neglected. Principally this is out of the scope

of this paper; the basic relationships are given in [6] and [7]. When designing smaller CAN FD networks targeting at higher baud rates (e.g. 2 Mbit/s) the rules for the data phase are the limiting factor in most cases, not the rules for Classical CAN. However in large networks (e.g. industrial applications) the limiting factor might be arbitration and not the CAN FD data phase.

## Design rules for CAN FD

The principals of the robustness of the CAN FD protocol concerning bit timing, clock tolerance and any kind of asymmetry of the received CAN signals have already been given in [2] and [3]. However these are theoretical values based on logic signals. Now the existing gap to real CAN FD topologies and practical implementations will be bridged!

The crucial point for Classical CAN systems is the interaction between transmitter and receiver (i.e. the delay of the signals), whereas the main limitation in CAN FD systems is the asymmetry of the received signals. The tolerable shrinking and growing of bits has been expressed in [3] as “phase margin”. Since dominant and recessive bits can either shrink or grow with different consequences for the protocol two values (PM1 and PM2) have been defined. These are depending on the chosen bit time settings shown in figure 1 for both values and different sample point positions in the range between 500 kbit/s and 2 Mbit/s. If the asymmetry of the received bits exceeds the values for PM1 or PM2 communication will break down.

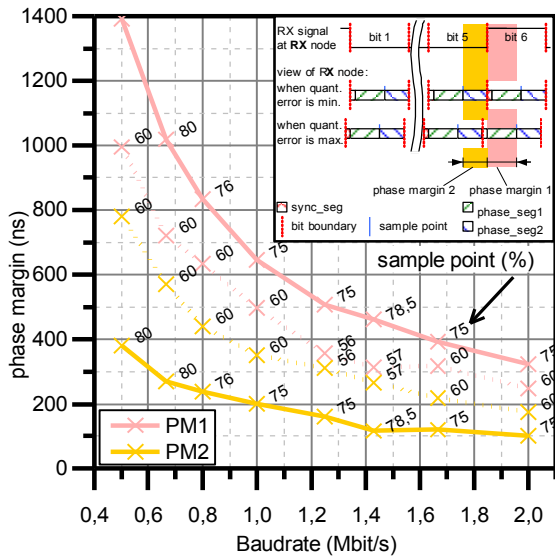


Figure 1: Phase margins for CAN FD

The phase margin in a real CAN system is the maximum allowable asymmetry before communication breaks down. To be sure that a CAN FD system will work properly under any circumstance all parts in a system that contribute to bit asymmetry have to be known including tolerances and varying operation conditions (e.g. temperature and aging). All these parts together must never exceed the phase margin. This is illustrated in figure 2.

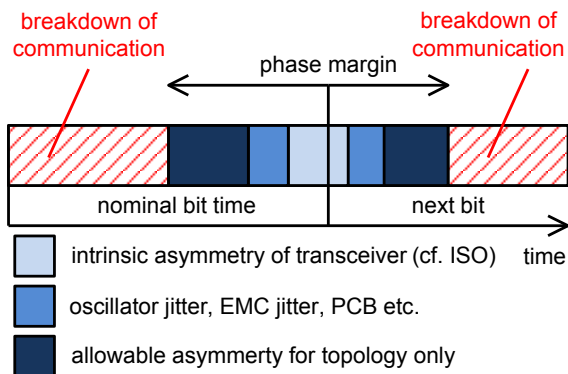


Figure 2: Distribution of phase margins

The allowed range of deviation from the nominal bit time of a single bit are the blue parts in figure 2, the red shaded area are the limits given by PM1 and PM2.

The first part which is inherent in any CAN or CAN FD system is the characteristics of the transceiver chips. Each transceiver has a typical delay and a typical asymmetry. Since transceiver timing characteristics spread depending on batch, temperature and aging it is recommended to use the limiting

values defined in DIS/ISO 11898-2:2015. A transceiver compliant to the ISO should not be worse. This part is marked light blue in figure 2.

The second part accounts for all other kind of asymmetries that are part of the physical layer not including the transceiver and the topology itself. It is subdivided into many smaller parts and it depends on the specific use case of the CAN FD system what to include and what values to take into consideration. In the following major values for typical automotive applications are given:

*Time interval error (TIE):* the clock of CAN FD controllers is usually derived from PLL circuits included in the  $\mu$ C. Any PLL is affected by phase noise causing a jitter between consecutive bits. This short term jitter is equivalent to bit asymmetry and it adds up to the overall asymmetry by a factor of four because a CAN bit is defined by two slopes at the transmitter side which have to be sampled at the receiver side (i.e. worst case: the first slope is delayed by transmitter and sampler at the receiver and vice versa for the second slope). Typical values are 5 ns ... 20 ns. Please note that the TIE is not equivalent to the static oscillator deviation which is already included in the calculation in [3] and which is mainly defined by the crystal being used.

*EMI jitter:* If a CAN or CAN FD system is exposed to EM radiation or fast common mode transients on the bus lines the RX signals provided by the receivers will be affected by jitter. Again this jitter will be seen by a controller as asymmetry of the received signal. It is difficult to define a distinct value for this, but EMI measurements have shown, that 50 ns is a reasonable value to account for this. However depending on the deployment of the system this might be less or even more.

*Logic asymmetry:* the signals exchanged between the state machine in the CAN FD controller and the transceiver (RX, TX) are also affected by asymmetry resulting from the input/output switching pads of the silicon chips and the PCB capacitance. The typical value for this is 10 ns for the transmitting and receiving node.

Finally the third part which is illustrated dark blue in figure 2 is the asymmetry caused by the topology, not including the transceivers. The assessment of this part will be treated in detail in the following chapters. Eventually it is recommended to account for future extensions of a network which means not to go directly to the limits of the phase margin when defining a new CAN FD system.

**Assessment of CAN FD topologies**

In order to estimate the asymmetry of a specific topology it is necessary to measure all communication relationships between all nodes included. This means to measure  $n^2$  signals if  $n$  is the number of nodes in the network. Since any CAN transmitter is simultaneously a receiver of his own signal, the so called “loop back” signals have to be considered as well. It is recommended to use varying test patterns in the message to find the worst case bit combination. In the end there will be one communication relationship with the highest asymmetry defining the worst case of the specific topology. This value has to be used for the calculation given above.

The principle of the measurement approach that has been used for all topology measurements is shown in figure 3. Basically the approach can be applied to simulation technology as well as to measurement

technology. In total approximately 750 different topology variations have been tested physically and analyzed automatically by software. In the end one point in the graphs of the next chapters represents the worst case asymmetry of an entire topology, i.e. one graph shows a set of characteristic curves consisting of many different topologies. The basic conditions of all measurements were: test message 2Mbit/s, transceiver NXPTJA1043T, room temperature, supply voltage  $5V \pm 5\%$ , choke  $51 \mu H$  bifilar, cable: FLRY  $2 \times 0,35 \text{ mm}^2$  (PVC standard CAN cable).

The assessment of the topologies is divided into four parts:

- Assessment based on the RX signal, split assessment of loop-back signal and signals from all other nodes.
- Assessment based on the bus signal at the respective node based at 500mV (D→R) and 900mV (R→D) threshold, split assessment of loop-back signal and signals from all other nodes. In the following this will be referred to as “virtual RX signal”.

An example for this is shown in figure 4 where the asymmetry of the received signal (blue lines) is determined twice, based on the RX signal (upper graph) and on the differential bus signal (lower graph).

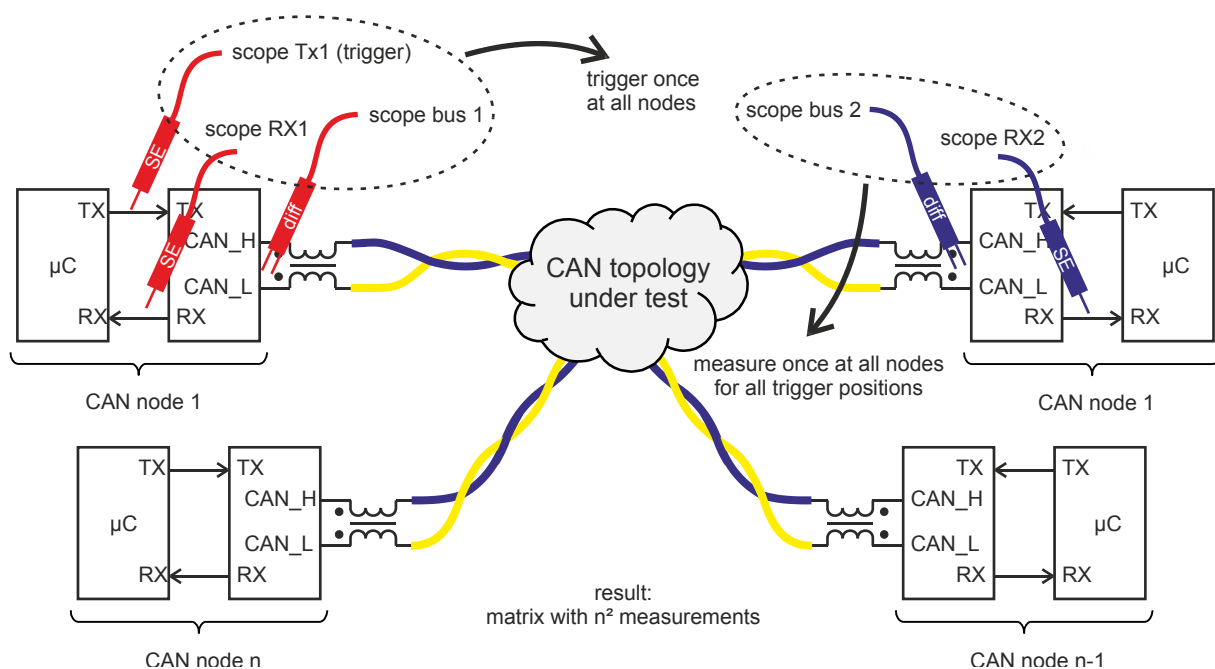


Figure 3: measurement approach for systematic topology assessment

The magenta circles depict the switching points of the virtual RX signal. This dual assessment is necessary since good transceivers are filtering out ringing on the bus fairly good with their hysteresis behavior. In many situations an improvement of the asymmetry on the RX pin can be observed paradoxically with increasing ringing to some extent. This can be deceiving for two reasons: Firstly the filtering of the ringing by the transceiver's hysteresis shows a distinct fall of the cliff behavior resulting in a jumping up asymmetry when reaching the limits of the hysteresis filtering. Secondly the filtering behavior is not specified in the DIS/ISO 11898-2:2015 which means that two unequal CAN transceiver implementations might behave differently while receiving CAN signals affected by ringing. Thus an assessment of a CAN topology should be based primarily on the bus signals and additionally on the RX signal delivered by a common CAN transceiver in order to guarantee stable and reproducible results. Finally it is up to the system designer to decide whether to trust in the RX signal or to consider the virtual RX signal based on thresholds of the differential bus signal. Finally it could be distinguished between asymmetry affecting PM1 and PM2 when evaluating the results.

If one of both dominates the appropriate setting of the sampling points could achieve an optimization of the system's reserves. However in this paper only the worst case is given not distinguishing between PM1 and PM2 in order not to dissipate one's energies in details, otherwise the number of graphs would have to be doubled.

It has to be pointed out, that the given topology measurements include the intrinsic asymmetry of an NXPTJA1043 transceiver at room temperature (approx. 20°C). If the worst case defined by the ISO shall be taken into account (which is recommended to consider temperature and aging effects), then the transceivers' typical values given in the datasheet by NXP have to be subtracted from the measured asymmetry values in a first step and in a second step the worst case asymmetry values given in the DIS/ISO 11898-2:2015 have to be added.

As a first approximation this represents the worst case asymmetry that could be expected from a topology. Please note that cables might change their parameters over temperature which would not be included in this approximation.

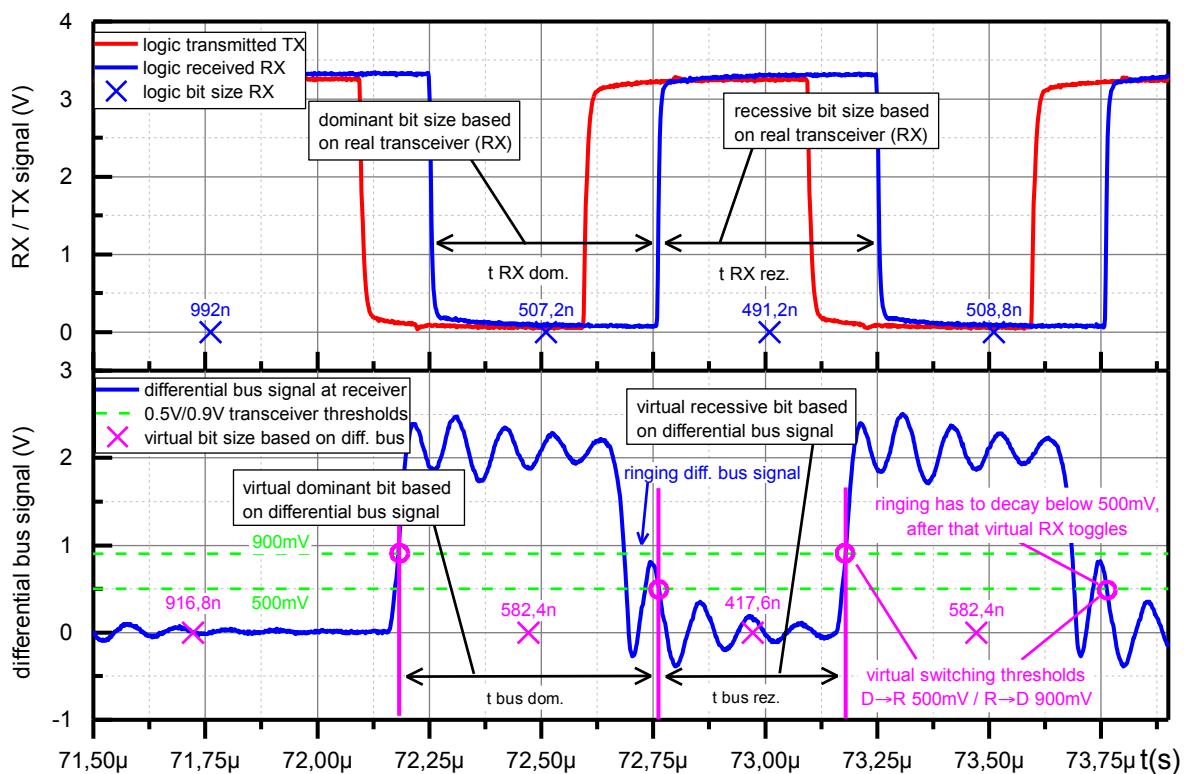


Figure 4: Definition of asymmetry based on real RX signal and „virtual” RX signal

### Point to point topology

This is the simplest topology in which two variations are possible: 1st terminated on both ends or 2nd terminated at one end.

Termination at one end is sometimes beneficial from a user point of view but not from a signal integrity point of view, as can be seen from the graphs in fig. 5. The measurement stops at approx. 30m because the communication broke down at this length at 2Mbit/s. Especially the loop back signal (i.e. the signal that is received by a transmitting node itself) is affected by strong ringing and therefore shows jumping up asymmetry with increasing line length.

If the point to point topology is terminated at both sides the asymmetry of the loop back signal remains on a low level basically

determined by the intrinsic asymmetry of the transceiver. The received signal at the other node shows increasing asymmetry with increasing line length mainly coming from the dispersion of the transmission line smoothing the slopes of the differential CAN signal. Anyhow long links are possible with a point to point topology. As standard PVC cable was used for this measurement the asymmetry could be improved a lot if a cable with lower dispersion would be used, e.g. FLR9Y (PP) or FLR2X (PE) instead of FLRY (PVC).

The assessment based on the RX and the virtual RX signals (i.e. the differential bus signal) are pretty similar in this case. As can be seen equally terminated point to point links are benchmark with regard to bit asymmetry.

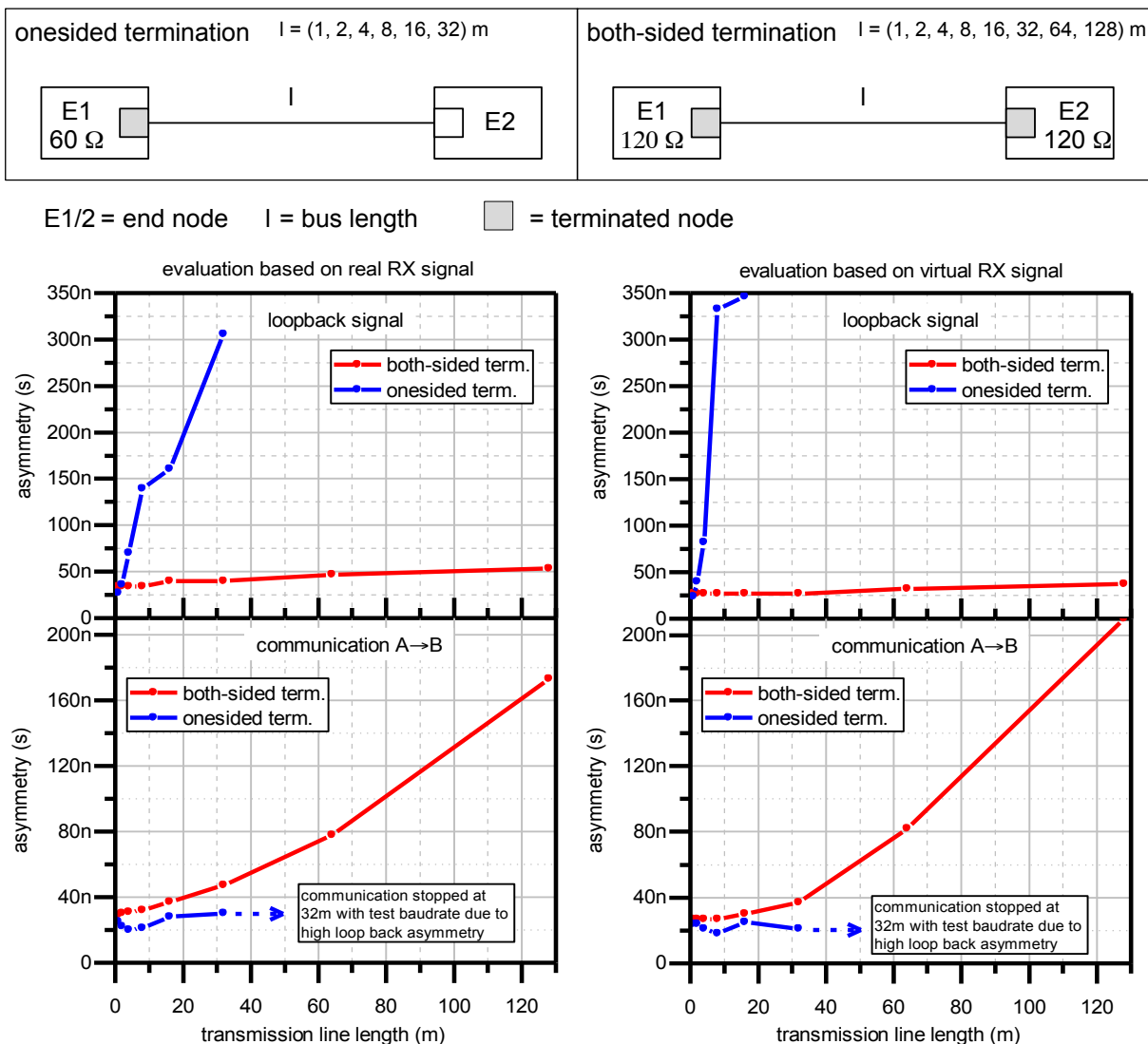


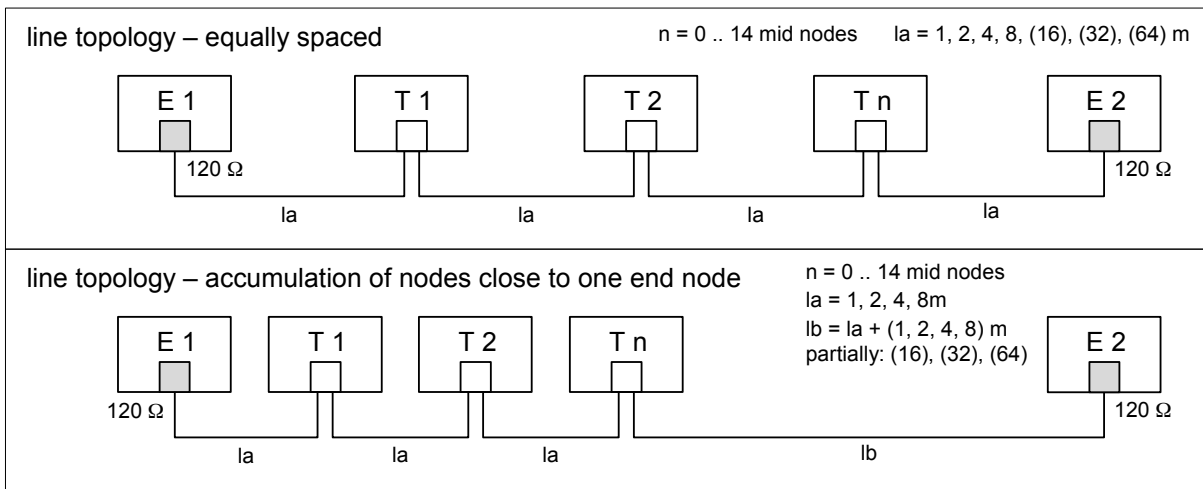
Figure 5: Asymmetry of point to point link

**Line topology**

The ideal line topology is frequently used in FlexRay systems. Basically it is a point to point link that is expanded with in-between nodes strictly avoiding stubs. This means that all nodes that are looped into the bus lines need 4 pins instead of 2. This is also the reason why this topology is quite unpopular. This topology has the advantage that it reduces reflections to a minimum. Sometimes this is also referred to as “daisy

chain topology” whereas this term is not appropriate in this context.

This topology has been investigated in different configurations: 1<sup>st</sup> equally spaced nodes, 2<sup>nd</sup> clustering of nodes at one end, 3<sup>rd</sup> clustering of nodes in the middle, 4<sup>th</sup> having multiple clusters and 5<sup>th</sup> random line distribution. In principle all five configurations show similar behavior for which reason only graphs for 1<sup>st</sup> and 2<sup>nd</sup> configuration are given.



E = end node    T = mid node    la/lb = line segment length     = terminated

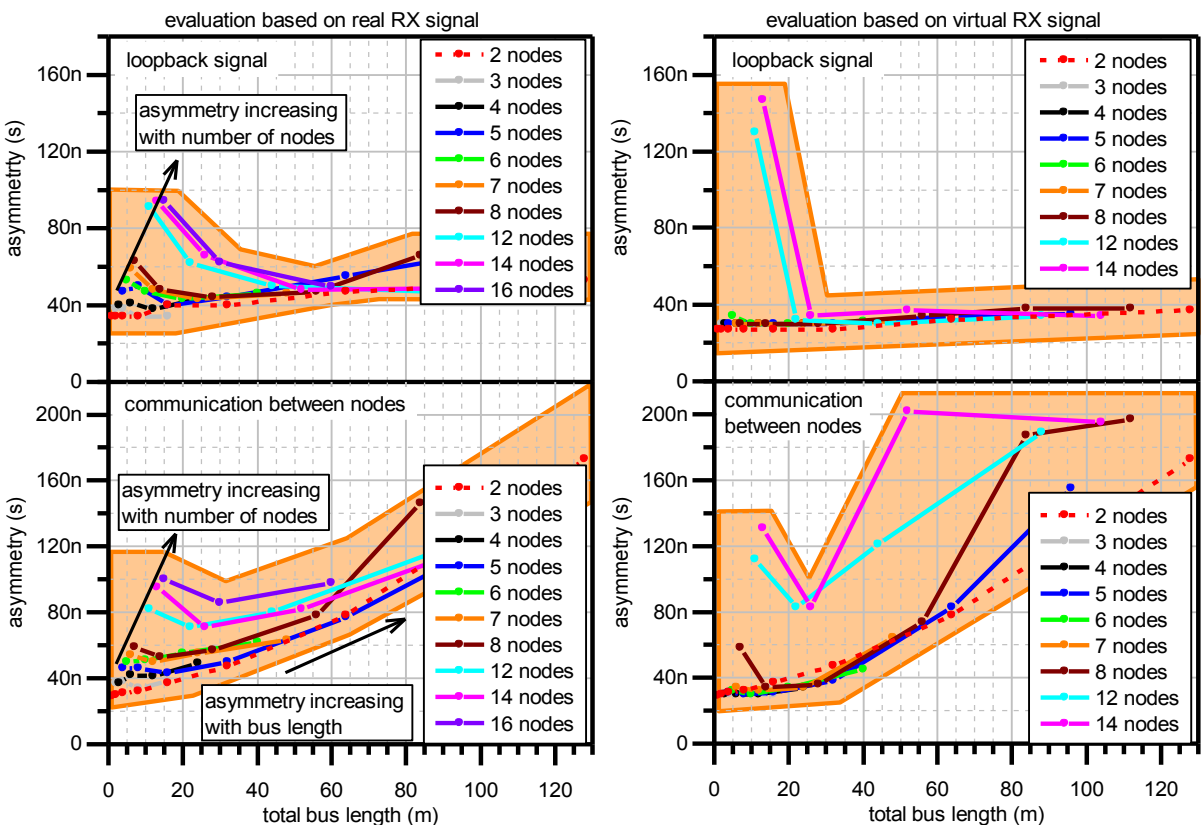


Figure 6: Asymmetry of line topology with equally spaced nodes

If the communication is evaluated based on the RX signal (fig. 6 on the left) it can be seen, that especially the loop back signal shows increasing asymmetry with increasing number of nodes at smaller transmission line lengths. This is due to fast ringing that occurs at the loop back signal of the in-between nodes and it becomes less if the bus line gets longer. The asymmetry of signals received from other nodes shows a similar behavior but at longer transmission line lengths the asymmetry rises continuously which is due to dispersion of the used transmission line. Again this effect could be improved if e.g. FLR9Y (PP) or FLR2X (PE) would be used instead of FLRY (PVC).

It can be observed, that all asymmetry values in figure 6 and following are all in a certain range. This is visualized by the colored area around the curves. All variations that have been tested lie within this area. It is very likely that variations of the topology that do not exceed the range of the tested variables (e.g. number of nodes, maximum line lengths) also lie within these areas, however this has not been tested. The colored areas should not be interpreted as strict boundary

values; they should give an overview and orientation to CANFD system designers.

If the evaluation is based on the virtual RX signal quite a similar behavior can be observed, however the spread is larger.

If nodes are clustered at one end of the bus having a distant end termination node the behavior is again very similar (fig. 7). The distance of the nodes within the cluster have nearly no influence on the asymmetry, though with rising distance of the end node the overall bus length grows which goes along with dispersion effects of the transmission line and increasing asymmetry.

In comparison to the topologies presented in the following chapters the line topology shows very little asymmetry. If it is built up in an appropriate manner strictly avoiding stubs and looping through the CAN signal through ECUs by means of 4 pins it has asymmetry values on the level of a point to point communication link. For CANFD systems targeting at high communication speed in the data phase this kind of topology is the most suitable.

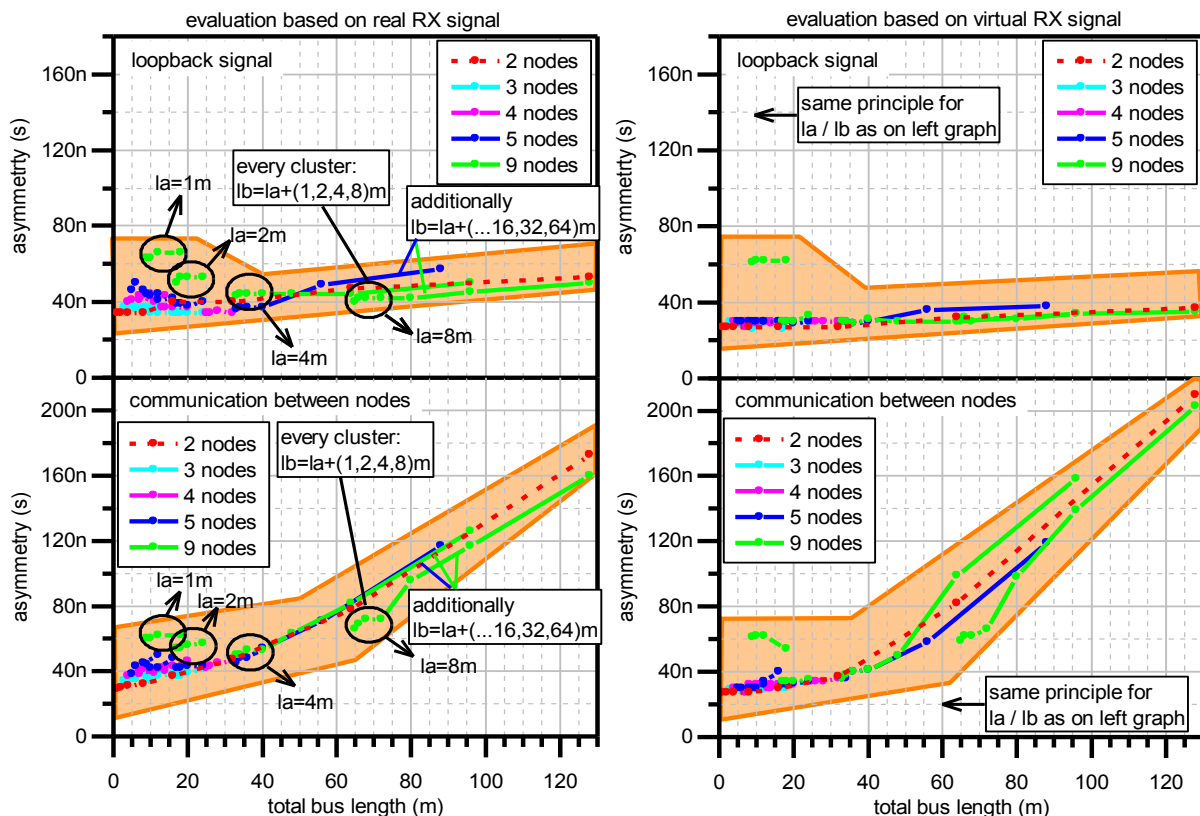
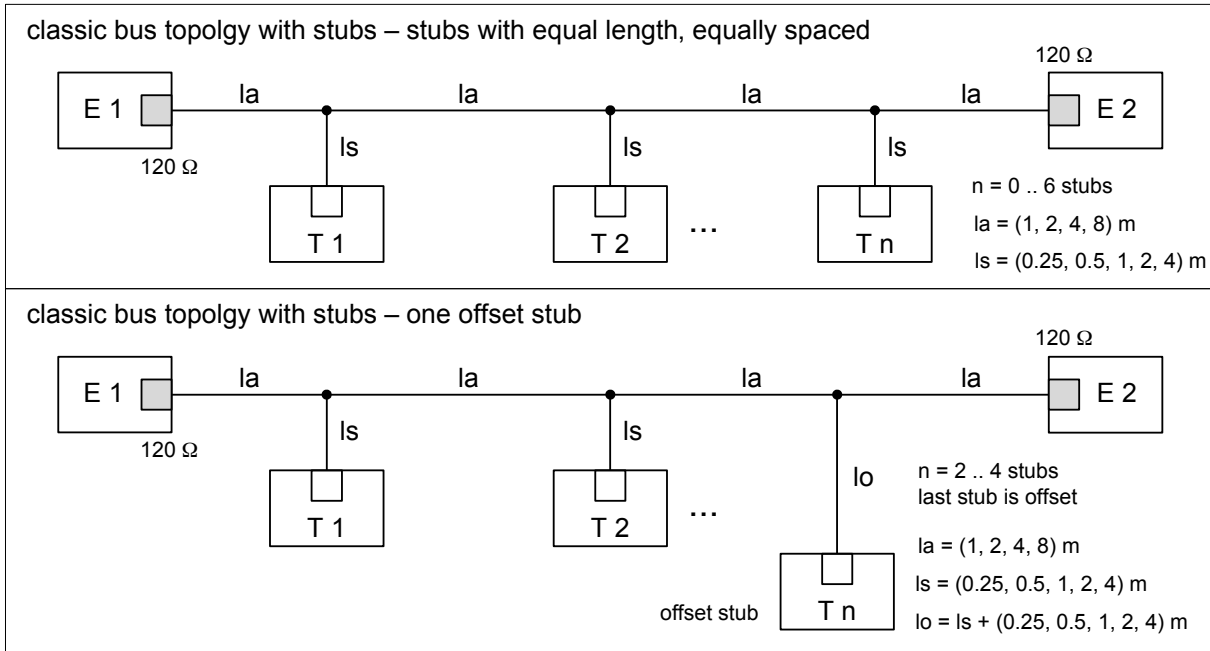


Figure 7: Asymmetry of line topology with clustered nodes

**Bus topology with stubs**

This may be the most popular and most frequently used CAN topology. The big question is how long the stubs can be since they are a source of reflections. The stub topology was investigated with 1<sup>st</sup> stubs of

equal length and equally spaced, 2<sup>nd</sup> same as 1<sup>st</sup> configuration but one of the stubs was offset and 3<sup>rd</sup> configuration were randomly distributed stubs of varying length. The last one is not included in the paper because the results were comparable to the first two configurations.



E = end node    T = mid node     $l_a/l_b$  = line segment length     $\square$  = terminated

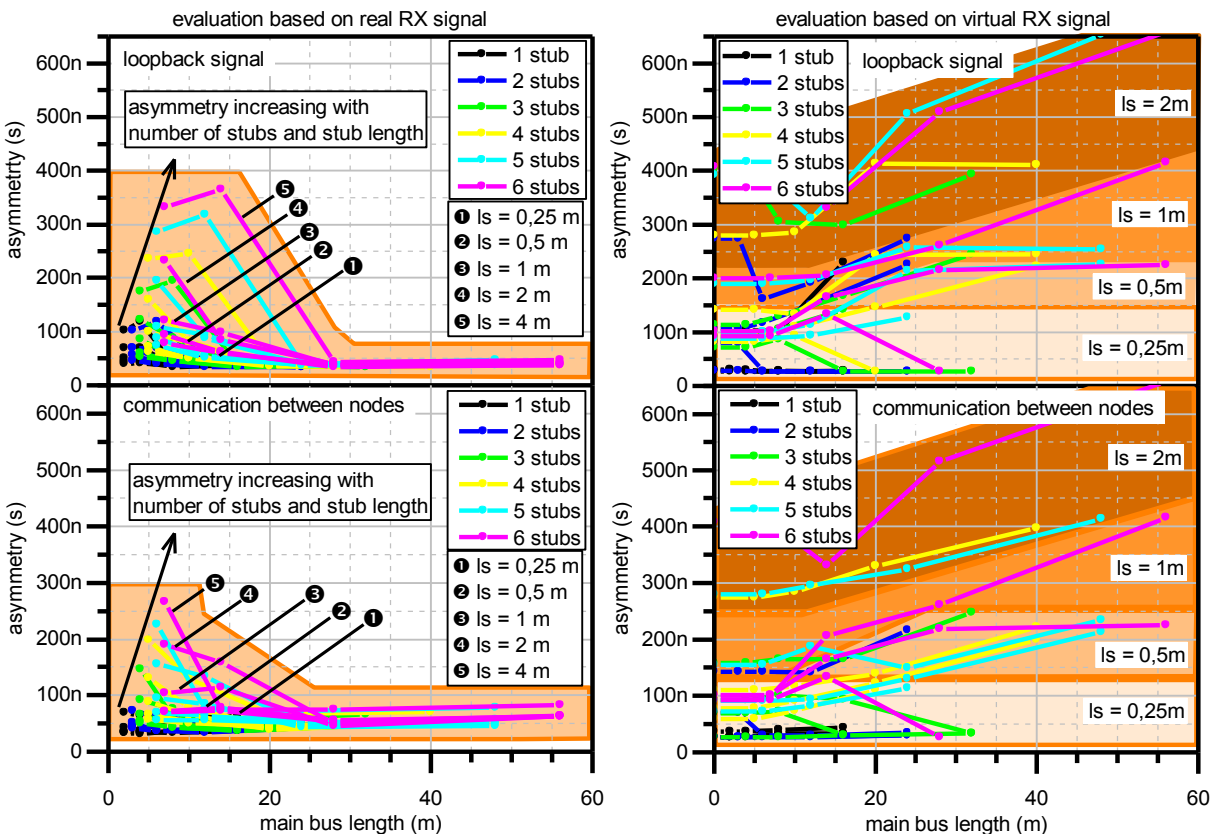


Figure 8: Asymmetry of bus topology with stubs of equal length, equally spaced



If the results are assessed based on the RX signal (fig.8 left) a pattern comparable to the line topology can be observed: an increasing asymmetry with an increasing number of nodes at smaller bus lengths. For larger bus lengths (in this case the total bus length was limited to a little less than 60m) the observed asymmetry seems to be surprisingly low, even if the stubs become quite long (e.g. 4m).

However if the assessment is based on the virtual RX signal (i.e. a bad receiver is assumed) completely contradictory properties of the topology regarding asymmetry can be seen (fig. 8 right). Especially with increasing stub length the asymmetry bounces up for both, loop back signal and communication between nodes. The dependency on the stub length is visualized in figure 8 right side by different shadings of the colored area.

An analysis of the differential bus signals shows that the stubs cause reflections that affect loop back signals as well as communication signals between nodes. The ringing frequency is dependent on the sub length and drops slower under the receiver

threshold with increasing stub length. This kind of topology is a good example for the capability of modern CAN transceivers to filter out ringing. However a system designer can only rely on that if the limits of the transceivers' filtering capabilities are well known. If this is not the case it is rather recommended to consider the virtual RX signal instead of the RX signal for system design.

Finally figure 9 shows the results if only one stub is lengthened and the other stubs maintain a stub length of 1m. The total asymmetry is less in this case however the principle relationships stay the same. More tests with randomly varying stub lengths and distance between the stubs also show similar behavior. A particularly bad situation has been found when multiple stubs are connected to the bus line at the same position.

Classic bus with stubs topologies are popular among many CAN system designers, however the given results show that this is not the optimum topology for CAN FD systems targeting at high communication speeds. If it should be used anyway for CAN FD keep the stubs as short as possible.

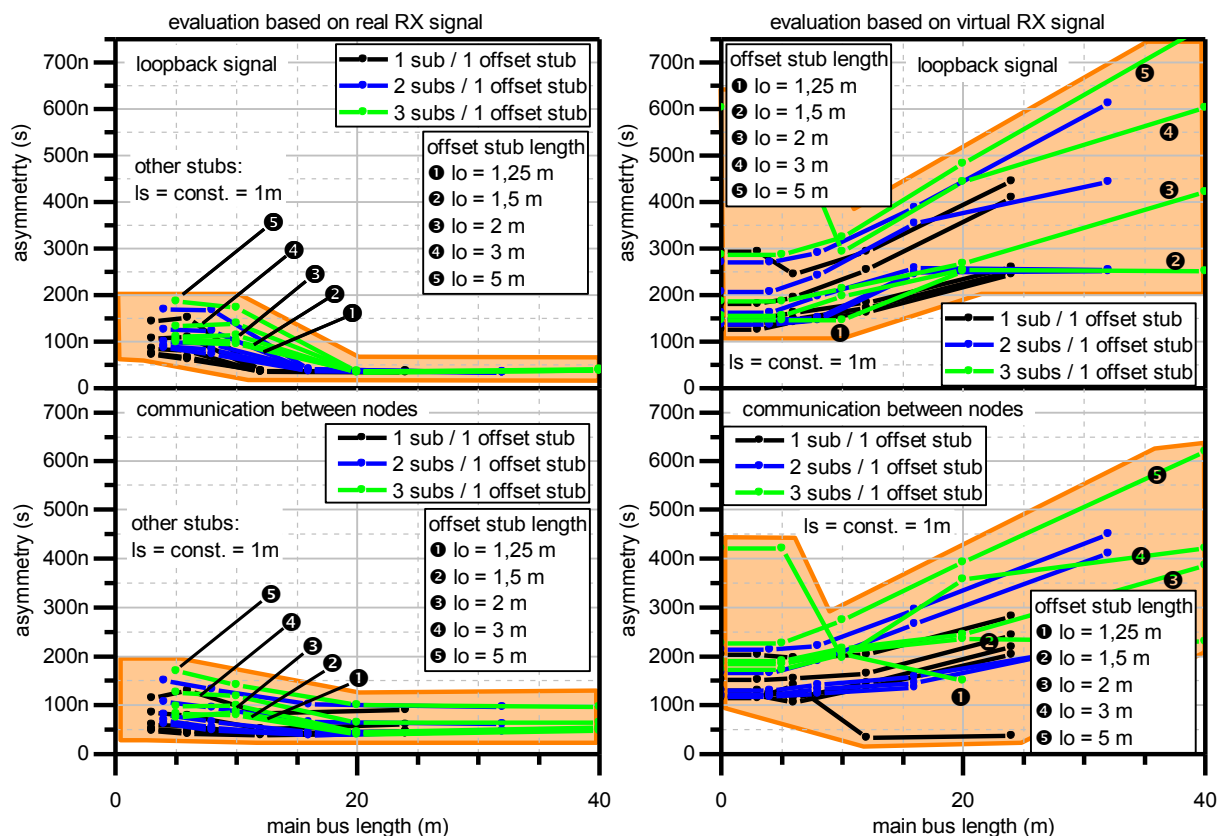


Figure 9: Asymmetry of bus topology with 1m stubs and one offset stub

**Star topology with ferrites**

The star topology used to be patented by Daimler-Benz in the 1990s (DE4235616) and thus it is mainly deployed in Daimler trucks, busses and passenger cars. The physical principle is shown in figure 10.

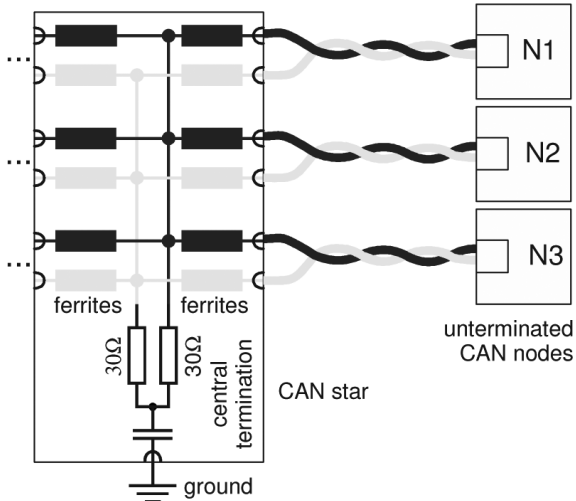


Figure 10: star topology principle

The main advantage of this configuration is that CAN nodes can be added or removed to a topology in a simple manner not disturbing the principal structure of the network. Since the patent is expired by now some other car makers use this kind of topology as well. The key point of this topology is the usage of ferrites deployed in the star center. Star topologies not using ferrites in the star center are only suitable for very low baud rates and thus they are not considered in this paper.

Different configurations of this topology have been tested. In the 1<sup>st</sup> configuration all

branches of the star are varied with equal length, 2<sup>nd</sup> half of the branches are extended in length and 3<sup>rd</sup> branches with equal length and one offset branch with extended length were tested. Since the last one shows similar results compared to the 2<sup>nd</sup> one, these graphs will be omitted.

First the assessment based on the RX signal is regarded. In figure 12 left the loop back asymmetry seems to be fairly low whereas the communication between nodes is affected by considerable asymmetry, which is rising with branch length and with the number of branches. Obviously the worst case is a large number of branches and longer branch lengths, however with few branches and moderate branch length low asymmetries still can be achieved. A similar result can be seen in figure 13 where short and long branches are combined. Please note that the maximum branch lengths in this case are longer than those in figure 12 which explains the overall higher asymmetry. A star topology will always be affected by reflections as well as stub topologies. That becomes evident when looking at the virtual RX signal that accounts for ringing on the bus. Especially for a higher number of nodes the asymmetry bounces up even at moderate branch lengths. In figure 12 many data points are missing for this case because an asymmetry value could not be defined anymore since the ringing persists for the whole bit time of the baud rate that was used for the measurements (2Mbit/s). Again this is a good example for the capability of modern transceivers to filter out ringing.

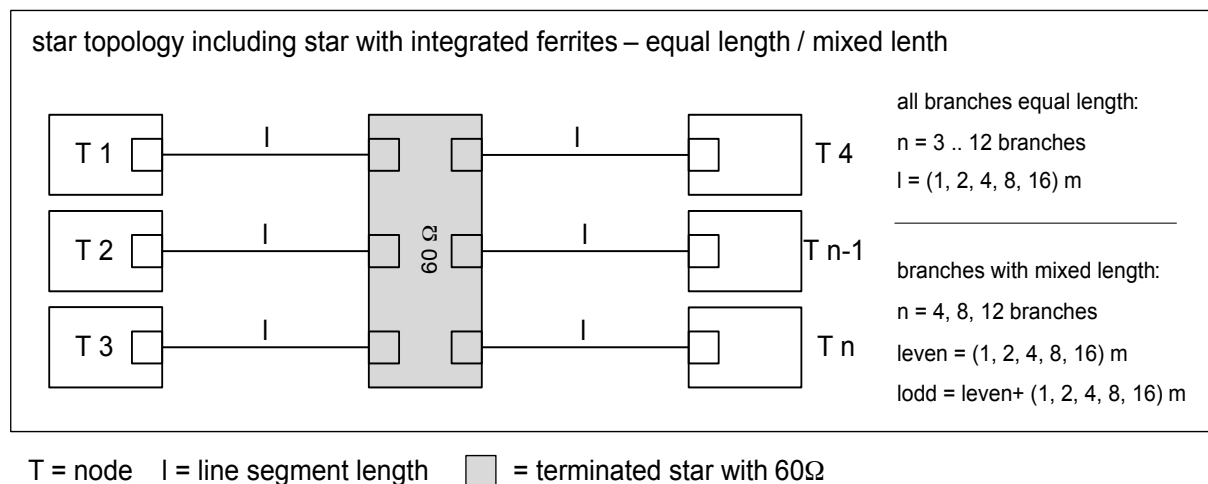


Figure 11: Star topology tested configurations

Anyhow there are configurations of the star topology (e.g. branches  $\leq 2\text{m}$  and no more than 8 nodes) where higher baud rates are possible, even if the virtual RX signal is used for estimation. However for general CAN FD system implementations the star topology is only applicable for baud rates which are in the range of Classical CAN.

## Conclusion

An extensive measurement series of different CAN FD topology structures with a lot of varying parameters has been performed. In the process, the CAN FD signal asymmetries have been analyzed based on the RX as well as on a virtual RX signal based on the differential bus signal. Although the number of assessed variations was huge (approximately 750 in total) of course they cannot cover all kinds of CAN FD topologies that might occur in the field. Nevertheless the given measurement results can give a good basic overview about the typical behavior of particular topologies and they might be a good help for a CAN FD system designer to configure CAN FD networks in an appropriate manner.

It should be noted that the presented results are valid only at room temperature. The inclusion of temperature dependent behavior would have doubled the number of graphs and would have gone far beyond the scope of this paper. Large changes over temperature have to be expected if PVC cable is used, otherwise the main influence comes from the transceivers which can be accounted for by applying the worst case ISO values.

If the CANFD system design is targeting at high baud rates in the data phase (e.g. 2Mbit/s or above) it is evident, that the best results can be achieved with the point to point and with the line topology. Especially for conservative system designers that do not want to tolerate the uncertainty of ringing in the network the pure line topology is the only safe choice.

Anyhow the popular bus with stubs topology can be used for CANFD, even at higher baud rates but in this case it is recommended to keep the stubs as short as possible

and rather increase the overall bus length than allowing for longer stubs. However the system designer has to live with the presence of ringing on the bus lines which has to be controlled carefully.

Eventually the ferrite star topology can handle fast CANFD signals but only with low branch lengths and a moderate number of branches. After all this kind of topology might be helpful to flexibly interconnect CANFD devices that are close to each other, e.g. multiple ECUs in an electric control cabinet. If baud rate doesn't matter the results show that the system designer has much more freedom to choose between different topology structures. The given graphs can be a source of orientation.

---

Dr.-Ing. Marc Schreiner  
Daimler AG – Research and Development  
Wilhelm-Runge-Straße 11  
DE-89081 Ulm

## References

- [1] CAN with Flexible Data-Rate - Florian Hartwich, CAN in Automation, iCC 2012, Neustadt an der Weinstraße
- [2] Bit time requirements for CANFD - Florian Hartwich, CAN in Automation, iCC 2013 Paris
- [3] Robustness of a CANFD Bus System – About Oscillator Tolerance and Edge Deviations – A. Mutter, iCC 2013 Paris
- [4] Safeguarding CANFD for applications in trucks - M. Schreiner, H. Leier, M. Zerzawy, T. Dunke and J. Dorner, CAN newsletter 3/2013
- [5] CANFD from an OEM point of view, M. Schreiner, H. Mahmoud, M. Huber S. Koç, J. Waldmann, CAN in Automation, iCC 2013 Paris and CAN Newsletter 2/2014
- [6] Berechnung des Bit Timings bei CAN Bus Systemen / Teil1 und Teil2 – Klaus Dietmayer, Elektronik 21/1997 und Elektronik 22/1997
- [7] The Configuration of the CAN Bit Timing – Florian Hartwich, 6th International CAN Conference 2nd to 4th November, Turin (Italy) 1999